

# Thermodynamics of rotating self-gravitating systems

E.V. Votyakov, A. De Martino and D.H.E. Gross

Hahn-Meitner-Institut, Bereich Theoretische Physik, Glienickerstr. 100, 14109 Berlin (Germany)

e-mail: votyakov@hmi.de, demartino@hmi.de, gross@hmi.de

**Abstract.** We investigate the statistical equilibrium properties of a system of classical particles interacting via Newtonian gravity, enclosed in a three-dimensional spherical volume. Within a mean-field approximation, we derive an equation for the density profiles maximizing the microcanonical entropy and solve it numerically. At low angular momenta, i.e. for a slowly rotating system, the well-known gravitational collapse “transition” is recovered. At higher angular momenta, instead, rotational symmetry can spontaneously break down giving rise to more complex equilibrium configurations, such as double-clusters (“double stars”). We analyze the thermodynamics of the system and the stability of the different equilibrium configurations against rotational symmetry breaking, and provide the global phase diagram.

**PACS.** 05.20.-y Classical statistical mechanics – 04.40.-b Self-gravitating systems – 64.60.Cn Order-disorder transformations; statistical mechanics of model systems

## 1 Introduction

In this article, we study the equilibrium properties of a system of  $N$  classical particles subject to mutual gravitation, assuming that this self-gravitating gas is enclosed in a finite three-dimensional spherical box and rotates around its center. The Hamiltonian reads

$$H_N \equiv H_N(\{\mathbf{r}_i\}, \{\mathbf{p}_i\}) = \frac{1}{2m} \sum_{i=1}^N p_i^2 + \Phi(\{\mathbf{r}_i\}) \quad (1)$$

$$\Phi(\{\mathbf{r}_i\}) = -Gm^2 \sum_{1 \leq i < j \leq N} \frac{1}{|\mathbf{r}_i - \mathbf{r}_j|} \quad (2)$$

where  $\mathbf{r}_i \in V \subset \mathbb{R}^3$ ,  $\mathbf{p}_i \in \mathbb{R}^3$  and  $m > 0$  denote, respectively, the position, momentum and mass of the  $i$ -th particle, while  $G$  is the gravitational constant. (In the following, we set  $m = 1$ .)  $V$  stands for the (volume of the) box containing the particles. Notice that the total potential energy scales as  $N^2$ . One wants

- a. to calculate the spatial distribution of particles at equilibrium, i.e. the most probable microscopic state;
- b. to derive the global phase diagram of the system;
- c. to study its thermodynamics (e.g. caloric curves);
- d. to describe the phase transitions that eventually take place.

In general, the physics of systems whose microscopic constituents interact via long-range potentials<sup>1</sup>, such as

<sup>1</sup> By which we will mean decaying with the interparticle distance  $r$  more slowly than  $r^{-D-\epsilon}$  with  $\epsilon > 0$  in  $D$  dimensions when  $r \rightarrow \infty$ .

(1,2), is highly non-standard and the analysis of their equilibrium state represents a considerable theoretical challenge [1]. At odds with more conventional systems with short-ranged forces, they are not additive (i.e. they cannot be divided into macroscopic subsystems with negligible mutual interaction) and not extensive (i.e. the densities of thermodynamic functionals are not bounded in the limit  $N \rightarrow \infty$ ). These facts have several important consequences. Long-range systems can have negative specific heat [2–6]; statistical ensembles can be inequivalent [5, 7–10]<sup>2</sup>; they do not possess a proper infinite-volume limit [11]; and they can attain inhomogeneous configurations (indeed, even their ground state is inhomogeneous, and it has been suggested that fractal structures may as well arise [12, 13]). Conventional statistical mechanics techniques that apply to homogeneous, short-range systems hence fail for long-range systems. The key theoretical problem here is a very fundamental one: to devise a mathematical framework that allows the study of phase transitions and other collective phenomena [14].

Self-gravitating gases are the most prominent example of a long-range system and have attracted a great deal of attention over the years. Most static theories rely on the microcanonical ensemble, where conserved macroscopic observables represent the natural control parameters (see [15] for a review). The task in this setting is that of finding the most probable (entropy-maximizing) equilibrium configuration of (1,2) with  $V$  finite as a func-

<sup>2</sup> In fact, the paper [5] pointed explicitly to the failure of the canonical ensemble near first-order phase transitions in general, and to its non-equivalence with the fundamental microcanonical ensemble, which displays a negative heat capacity there.

tion of the integrals of (Hamiltonian) motion, the simplest and physically most relevant being the total energy  $E$  and the total angular momentum  $\mathbf{L} = \sum_{i=1}^N \mathbf{r}_i \times \mathbf{p}_i$ , whose conservation is related to the invariance of (1) under rotations. Taking the conservation of  $\mathbf{L}$  into account leads however to enormous technical difficulties. Most authors have thus neglected rotation by breaking the rotational symmetry explicitly from the outset, e.g. by taking a non-spherical  $V$ , and used  $E$  as the only control parameter (see e.g. [16–18] for some recent work). The analysis of the equilibrium state of self-gravitating gases is hence a rather well-studied problem without rotation. It turns out that at high energy (i.e. temperature), where the kinetic term dominates, the system is most likely found in a homogeneous cloud (shortly, “gas” state) filling the available volume. At low energy, instead, where the gravitational energy dominates, a collapsed configuration is preferred, where particles form a single dense globular cluster lying in an almost void background (“single star”). This is the well-known gravitational collapse transition first described in [19]. In between these two “phases” (not being homogeneous, the single-cluster is not a proper thermodynamic phase), for a whole range of energies, the specific heat is negative. In this transition regime the canonical ensemble fails<sup>3</sup>.

For a rotating system, the situation is expected to be substantially more complex. From a qualitative viewpoint, the equilibrium density profile will depend on the ratio between the rotational and gravitational contributions to the total energy. When the latter dominates, gravitational attraction should cause the system to collapse. At high ratios, instead, when rotation is sufficiently fast (high angular momentum), more complex distributions should arise. Dynamical studies based on fluid-mechanics techniques [21–23] suggest that ring-like and disk-like structures might appear. Ultimately, at sufficiently high rotational energies, two distinct dense clusters (i.e. a “double star”) should form.

The richness suggested by the fluid-dynamical picture cannot be recovered in a static equilibrium theory without the inclusion of rotation. Double-cluster configurations can arise in a static framework only from the spontaneous breaking of the rotational symmetry of (1), which should take place when the angular momentum is sufficiently high. Effects connected to rotation should also lead to the formation of rings and other types of structures. Despite some attempts [24, 25], however, a detailed static theory embodying angular momentum is lacking.

The purpose of this work, which builds on [21, 25], is to include angular momentum in the microcanonical theory. Using a mean-field approximation, we derive an integral equation for the density profiles corresponding to stationary points of the microcanonical entropy surface and solve it numerically as a function of  $E$  and  $L = |\mathbf{L}|$ . The usual collapse transition is recovered at low angular momentum. At high angular momenta, instead, we find that

a spontaneous breakdown of the rotational symmetry occurs at sufficiently low energies. This gives rise to more complex equilibrium structures, including “double stars”, rings and disks. We derive the global phase diagram of the self-gravitating gas in the  $(E, L)$  plane. By studying the Hessian of the microcanonical entropy [9, 26], we characterize three pure phases (where the system is found in a “gas”, “single star” and “double star” configuration, respectively) and a large mixed phase with negative specific heat, phase separation and competition between different equilibrium density profiles. Finally, we analyze the thermodynamics of the system, deriving the caloric curves (temperature versus energy) in the different phases, and analyze the stability of the stationary distributions.

This paper, which follows [27], is structured as follows. In Sec. 2 we expose the microcanonical mean field theory of (1), derive the entropy functional and the stationarity condition. Sec. 3 is dedicated to the results. We report the numerical solution of the main equation, together with the global phase diagram and a few equilibrium configurations. Then we pass to the thermodynamics of the system, with special emphasis on the rotational-symmetry-breaking transition, the physics of mixed phase, and the stability problem. Finally, Sec. 4 contains our conclusions and a some remarks about the work presented here, and a list of open problems.

## 2 Microcanonical mean-field theory

We consider the system with Hamiltonian as given in (1,2), enclosed in a three-dimensional spherical volume  $V$ , to preserve rotational symmetry and ensure conservation of the total angular momentum  $\mathbf{L}$ . At the same time, the box breaks translational invariance, hence the total linear momentum is not conserved. The aim of the microcanonical theory is to find the particles’ density profiles  $\rho(\mathbf{r})$  satisfying

$$\int_V \rho(\mathbf{r}) d\mathbf{r} = N \quad (3)$$

that maximize the entropy ( $k = 1$ )

$$S_N(E, \mathbf{L}) = \ln W_N(E, \mathbf{L}) \quad (4)$$

$W_N$  being the microcanonical “partition sum” ( $h = 1$ )

$$W_N(E, \mathbf{L}) = \frac{\epsilon}{N!} \int \delta(H_N - E) \delta(\mathbf{L} - \sum_{i=1}^N \mathbf{r}_i \times \mathbf{p}_i) D\mathbf{r} D\mathbf{p} \quad (5)$$

We used the shorthand notations  $D\mathbf{r} = \prod_{i=1}^N d\mathbf{r}_i$  and  $D\mathbf{p} = \prod_{i=1}^N d\mathbf{p}_i$ .  $\epsilon$  is a constant that makes  $W_N$  dimensionless. Integrals over momenta are from  $-\infty$  to  $+\infty$ , while integrals over  $\{\mathbf{r}_i\}$  are performed over  $V^N$ . Clearly, such equilibrium profiles will depend on  $E$  and  $\mathbf{L}$ .

We now calculate the microcanonical partition sum (5). To perform the integrals over momenta, namely to

<sup>3</sup> It has been recently shown that ensemble equivalence is restored in the “dilute” limit  $(N, V) \rightarrow \infty$  with  $N/V^{1/3}$  fixed, in which thermodynamic functionals exist [20].

evaluate

$$F_N(\{\mathbf{r}_i\}, K, \mathbf{L}) = \int \delta(K - \frac{1}{2} \sum_{i=1}^N p_i^2) \delta(\mathbf{L} - \sum_{i=1}^N \mathbf{r}_i \times \mathbf{p}_i) D\mathbf{p} \quad (6)$$

one can follow Laliena [25] (see also [9]) and use the Laplace transform of  $F_N$  in  $K$ , that is ( $\Re s > 0$ )

$$\tilde{F}_N(\{\mathbf{r}_i\}, s, \mathbf{L}) = \int_0^\infty F_N(\{\mathbf{r}_i\}, K, \mathbf{L}) e^{-sK} dK \quad (7)$$

Inserting the integral representation of the  $\delta$  function and performing the trivial integral over  $K$  one gets

$$\tilde{F}_N(\{\mathbf{r}_i\}, s, \mathbf{L}) = \int e^{i\boldsymbol{\omega} \cdot \mathbf{L} - i \sum_i \boldsymbol{\omega} \cdot \mathbf{r}_i \times \mathbf{p}_i - \frac{s}{2} \sum_i p_i^2} D\mathbf{p} D\boldsymbol{\omega} \quad (8)$$

where  $D\boldsymbol{\omega} = d\boldsymbol{\omega}/(2\pi)^3$ . The above integrals are at most of Gaussian type and can be performed to yield

$$\tilde{F}_N(\{\mathbf{r}_i\}, s, \mathbf{L}) = \frac{(2\pi)^{\frac{3N-3}{2}}}{\sqrt{\det \mathbb{I}}} \frac{e^{-\frac{1}{2} s \mathbf{L}^T \mathbb{I}^{-1} \mathbf{L}}}{s^{\frac{3N-3}{2}}} \quad (9)$$

where  $\mathbb{I} \equiv \mathbb{I}(\{\mathbf{r}_i\})$  denotes the inertia tensor, with elements ( $a, b = 1, 2, 3$ )

$$I_{ab}(\{\mathbf{r}_i\}) = \sum_{i=1}^N (r_i^2 \delta_{ab} - r_{i,a} r_{i,b}) \quad (10)$$

and  $\mathbf{L}^T \mathbb{I}^{-1} \mathbf{L} = \sum_{a,b} L_a I_{ab}^{-1} L_b$ . The inverse Laplace transform of (9) is given by

$$F_N(\{\mathbf{r}_i\}, K, \mathbf{L}) = \frac{(2\pi)^{\frac{3N-3}{2}}}{\Gamma(\frac{3N-3}{2}) \sqrt{\det \mathbb{I}}} (K - \frac{1}{2} \mathbf{L}^T \mathbb{I}^{-1} \mathbf{L})^{\frac{3N-5}{2}} \quad (11)$$

for  $K > \frac{1}{2} \mathbf{L}^T \mathbb{I}^{-1} \mathbf{L}$  and  $F_N(\{\mathbf{r}_i\}, K, \mathbf{L}) = 0$  otherwise. Hence after integrating out the momenta the microcanonical partition function reads

$$W_N(E, \mathbf{L}) = \frac{\epsilon A}{N!} \int \frac{[E - \frac{1}{2} \mathbf{L}^T \mathbb{I}^{-1} \mathbf{L} - \Phi(\{\mathbf{r}_i\})]^{\frac{3N-5}{2}}}{\sqrt{\det \mathbb{I}}} D\mathbf{r} \quad (12)$$

where  $A = (2\pi)^{\frac{3N-3}{2}} / \Gamma((3N-3)/2)$ . The term in square brackets in (12) is nothing but the kinetic energy of the system. Now setting for simplicity  $\mathcal{K} = E - \frac{1}{2} \mathbf{L}^T \mathbb{I}^{-1} \mathbf{L} - \Phi(\{\mathbf{r}_i\})$ , we remark that the integrand is

$$e^{N[\frac{3}{2} \log \mathcal{K} - \frac{5}{2N} \log \mathcal{K} - \frac{1}{2N} \log \sqrt{\det \mathbb{I}}]} \quad (13)$$

Being interested in the behaviour of the system for large  $N$  (see below), we shall retain just the leading order in  $N$  in the above expression. We are thus left with

$$W_N(E, \mathbf{L}) = \frac{\epsilon A}{N!} \int [E - \frac{1}{2} \mathbf{L}^T \mathbb{I}^{-1} \mathbf{L} - \Phi(\{\mathbf{r}_i\})]^{\frac{3N}{2}} D\mathbf{r} \quad (14)$$

and it remains to integrate over  $V^N$ .

To this aim, we write the potential  $\Phi$  and the components of the inertia tensor as functionals of the density profile  $\rho$  as follows:

$$\Phi(\{\mathbf{r}_i\}) \rightarrow \Phi[\rho] = -\frac{G}{2} \int \frac{\rho(\mathbf{r})\rho(\mathbf{r}')}{|\mathbf{r} - \mathbf{r}'|} d\mathbf{r} d\mathbf{r}' \quad (15)$$

$$I_{ab}(\{\mathbf{r}_i\}) \rightarrow I_{ab}[\rho] = \int \rho(\mathbf{r}) (r^2 \delta_{ab} - r_a r_b) d\mathbf{r} \quad (16)$$

Notice that in this way two- and many-body correlations are neglected. This allows to recast (17) in the form of the functional-integral

$$W_N^{\text{mf}}(E, \mathbf{L}) = \frac{\epsilon A}{N!} \int [E - \frac{1}{2} \mathbf{L}^T \mathbb{I}^{-1} \mathbf{L} - \Phi[\rho]]^{\frac{3N}{2}} P[\rho] d\rho(\mathbf{r}) \quad (17)$$

(mf = mean field) where  $P[\rho]$  is the probability to observe a density profile  $\rho \equiv \rho(\mathbf{r})$ . To estimate the latter, we follow the logic of Lynden-Bell [21]. We subdivide the spherical volume  $V$  into  $K$  identical cells labeled by the positions of their centers. The idea is to replace the integral over  $V^N$  with a sum over the cells. In order to avoid configurations with high densities where other physical processes (e.g. nuclear reactions) become more important than gravity, and cure the short-distance singularity of the Newtonian potential, we assume that each cell may host up to  $n_0$  particles ( $1 \ll n_0 \ll N$ ). This condition is essentially equivalent to considering hard spheres instead of point particles.  $P[\rho]$  is now proportional to the number of ways in which our  $N$  particles can be distributed inside the  $K$  cells with maximal capacity  $n_0$ . Denoting by  $n(\mathbf{r}_k)$  the number of particles located inside the  $k$ -th cell, a simple combinatorial reasoning leads to

$$P[\rho] \propto \frac{N!}{n(\mathbf{r}_1)! \cdots n(\mathbf{r}_K)!} \prod_{\text{cells } k} \frac{n_0!}{(n_0 - n(\mathbf{r}_k))!} = N! \prod_{\text{cells } k} \binom{n_0}{n(\mathbf{r}_k)} \quad (18)$$

where it is understood that the product involves configurations  $\{n(\mathbf{r}_k)\}$  such that  $\sum_k n(\mathbf{r}_k) = N$ . Introducing the relative cell occupancy

$$c(\mathbf{r}) = \frac{n(\mathbf{r})}{n_0} = \frac{V\rho(\mathbf{r})}{K n_0} \quad (19)$$

and approximating the factorials by means of Stirling's formula (assuming  $n(\mathbf{r}_k) \gg 1$  and  $n_0 - n(\mathbf{r}_k) \gg 1$ ), we get

$$P[c] \propto N! e^{-\frac{n_0 K}{V}} \int [c(\mathbf{r}) \log c(\mathbf{r}) + (1-c(\mathbf{r})) \log(1-c(\mathbf{r}))] d\mathbf{r} = N! e^{-\frac{N}{\Theta}} \int [c(\mathbf{x}) \log c(\mathbf{x}) + (1-c(\mathbf{x})) \log(1-c(\mathbf{x}))] d\mathbf{x} \quad (20)$$

where we introduced the dimensionless variable  $\mathbf{x} = \mathbf{r}/R$  and defined the average coverage

$$\Theta = \frac{NV}{n_0 K R^3} = \int c(\mathbf{x}) d\mathbf{x} \quad (21)$$

It is simple to check that in terms of  $c(\mathbf{x})$  the potential and the inertia tensor are respectively given by

$$\Phi[c] = -\frac{GN^2}{2R\Theta^2} \int \frac{c(\mathbf{x})c(\mathbf{x}')}{|\mathbf{x} - \mathbf{x}'|} d\mathbf{x}d\mathbf{x}' \quad (22)$$

$$I_{ab}[c] = \frac{NR^2}{\Theta} \int c(\mathbf{x})(x^2\delta_{ab} - x_ax_b)d\mathbf{x} \quad (23)$$

In the following, we shall measure energies in units of  $\frac{GN^2}{R}$  and inertia tensor components in units of  $NR^2$  so that we will be dealing with the reduced (dimensionless) quantities

$$\Phi[c] = -\frac{1}{2\Theta^2} \int \frac{c(\mathbf{x})c(\mathbf{x}')}{|\mathbf{x} - \mathbf{x}'|} d\mathbf{x}d\mathbf{x}' \quad (24)$$

$$I_{ab}[c] = \frac{1}{\Theta} \int c(\mathbf{x})(x^2\delta_{ab} - x_ax_b)d\mathbf{x} \quad (25)$$

Plugging (20) into (17), one arrives at the familiar form

$$W_N^{\text{mf}}(E, \mathbf{L}) \propto \int e^{NS_N^{\text{mf}}[c]} dc(\mathbf{x}) \quad (26)$$

where the “action”  $S_N^{\text{mf}}$  has the following expression:

$$\begin{aligned} S_N^{\text{mf}}[c] = & \frac{3}{2} \log \left[ E - \frac{1}{2} \mathbf{L}^T \mathbb{I}^{-1} \mathbf{L} - \Phi[c] \right] + \\ & - \frac{1}{\Theta} \int [c(\mathbf{x}) \log c(\mathbf{x}) + (1 - c(\mathbf{x})) \log(1 - c(\mathbf{x}))] d\mathbf{x} \end{aligned} \quad (27)$$

Clearly,  $\mathbb{I} \equiv \mathbb{I}[c]$ .  $S_N^{\text{mf}}$  has an obvious physical interpretation as the sum of the energetic and combinatorial contribution to the entropy, respectively. For large  $N$ , the integral (26) can be computed as usual by the steepest-descent (Laplace) method. This immediately yields

$$W_N^{\text{mf}}(E, \mathbf{L}) \simeq \exp \left[ N \max_{c(\mathbf{x})} S_N^{\text{mf}}[c] \right] \quad (28)$$

hence the “physical” value of the entropy density for large  $N$  is nothing but the maximum of  $S_N^{\text{mf}}$  over the space of relative cell occupancies  $c$ .

An elementary variation of  $S_N^{\text{mf}}$  with respect to  $c$ , the constraint on  $\Theta$  being enforced by a Lagrange multiplier  $\mu$  playing the role of a chemical potential, straightforwardly leads to the stationarity condition

$$\log \frac{c(\mathbf{x})}{1 - c(\mathbf{x})} = -\frac{\beta}{\Theta} U(\mathbf{x}) + \frac{1}{2} \beta (\boldsymbol{\omega} \times \mathbf{x})^2 - \mu \quad (29)$$

or, equivalently,

$$c(\mathbf{x}) = (1 + e^{\frac{\beta}{\Theta} U(\mathbf{x}) - \frac{1}{2} \beta (\boldsymbol{\omega} \times \mathbf{x})^2 + \mu})^{-1} \quad (30)$$

where  $\boldsymbol{\omega} \equiv \boldsymbol{\omega}[c]$  is the angular velocity (related to the total angular momentum by the relation  $\mathbf{L} = \mathbb{I}\boldsymbol{\omega}$ ), and  $\beta \equiv \beta[c]$  and  $U(\mathbf{x})$  are respectively defined as

$$\beta = \frac{3/2}{[E - \frac{1}{2} \mathbf{L}^T \mathbb{I}^{-1} \mathbf{L} - \Phi[c]]} \equiv \frac{3}{2K} \quad (31)$$

$$U(\mathbf{x}) = - \int \frac{c(\mathbf{x}')}{|\mathbf{x} - \mathbf{x}'|} d\mathbf{x}' \equiv 2\Theta^2 \frac{\delta \Phi}{\delta c(\mathbf{x})} \quad (32)$$

One sees that  $\beta$  is related to the kinetic energy of the systems, i.e. to the (inverse) temperature. The essence of the mean-field approximation is clearly expressed by the fact that

$$\Phi[c] = \frac{1}{2\Theta^2} \int c(\mathbf{x}) U(\mathbf{x}) d\mathbf{x} \quad (33)$$

Equation (29) (or (30)) is our central result. Functions  $c^*$  solving (29) and being entropy maxima in the space of  $c$ 's represent our desired equilibrium distribution of particles.

The correct way to analyze the problem consists in solving (29) at fixed energy and angular momentum, subsequently calculating intensive quantities (temperature and angular velocity). For the sake of simplicity and without any loss of generality, we now fix the angular momentum to lie parallel to the 3-axis, and concentrate on  $|\mathbf{L}| = L$ . We remark at this point that Lynden-Bell statistics, which is reminiscent of Fermi-Dirac statistics in real space (i.e. not in phase space), plays a crucial role. In fact, once overlapping is ruled out, the Hamiltonian (1) has a well-defined ground state, with particles collapsed in a core but without coming too close to each other. If one used Boltzmann statistics and point particles, instead, the system would have no ground state, since the potential energy would be unbounded from below. Antonov catastrophe [19] can be seen as a direct consequence of this fact. For this reason, Lynden-Bell statistics is probably more appropriate for self-gravitating systems<sup>4</sup>. The existence of a ground state ensures that (29) will always have a solution at fixed  $E$  and  $L$ . Of course, there may be multiple viable solutions at the same  $E$  and  $L$ , each bearing its entropy. In such a case, the criterion is simply that the higher the entropy, the more probable the solution.

Upon varying  $E$  and  $L$ , one can explore different regions of the parameter space and ultimately obtain the global phase diagram in the whole  $(E, L)$  plane. The main effect one expects from the inclusion of rotation is that, for sufficiently high angular momenta, upon decreasing the energy from high values, rotationally-symmetric solutions (e.g. homogeneous clouds) will become unstable against fluctuations that break rotational symmetry, and solutions without rotational symmetry (e.g. “double stars”) will bifurcate continuously from them.

The main problem at this point is merely technical. One can only hope to solve (29) or (30) by numerical integration. However, the implicit dependence of  $U(\mathbf{x})$  and  $\beta$  on  $c(\mathbf{x})$  via the three-dimensional integral (32) makes this a formidable task. Similar considerations hold for  $\boldsymbol{\omega}$ , which has to be computed from the relation  $\mathbf{L} = \mathbb{I}\boldsymbol{\omega}$ . To simplify things and in particular to reduce the dimensionality of the integrals involved, we pass to spherical coordinates,  $\mathbf{x} = (x, \theta, \phi)$ , and expand the Newtonian potential

<sup>4</sup> In order to restore a ground state, however, the Thirring potential [3], which mimics Newtonian gravity, has been used together with Boltzmann statistics (see e.g. [25]).

in series of real spherical harmonics (see e.g. [28]):

$$\frac{1}{|x - x'|} = \sum_{l=0}^{\infty} \sum_{m=-l}^l \frac{4\pi}{2l+1} \frac{(x \vee x')^l}{(x \wedge x')^{l+1}} Y_{lm}(\theta, \phi) Y_{lm}(\theta', \phi') \quad (34)$$

with  $x \vee x' = \min\{x, x'\}$  and  $x \wedge x' = \max\{x, x'\}$ . At the same time, we formally expand also the relative occupancy  $c$ :

$$c(\mathbf{x}) = \sum_{l=0}^{\infty} \sum_{m=-l}^l b_{lm}(x) Y_{lm}(\theta, \phi) \quad (35)$$

$b_{lm}(x)$  is a radial function whose precise form we will have to derive. Using the above series, together with the completeness relation for our basis set  $\{Y_{lm}\}$ ,

$$\int Y_{lm}(\theta, \phi) Y_{l'm'}(\theta, \phi) d\cos\theta d\phi = \delta_{ll'} \delta_{mm'} \quad (36)$$

one can easily show that

$$U(\mathbf{x}) = \sum_{l,m} u_{lm}(x) Y_{lm}(\theta, \phi) \quad (37)$$

$$u_{lm}(x) = -\frac{4\pi}{2l+1} \int \frac{(x \vee x')^l}{(x \wedge x')^{l+1}} b_{lm}(x') (x')^2 dx' \quad (38)$$

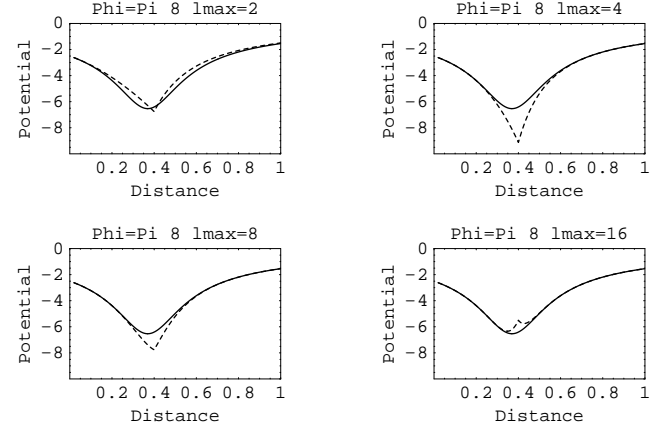
Multiplying both sides of (30) by  $Y_{lm}$  and integrating over angular variables one obtains for  $b_{lm}$  the system of integral equations

$$b_{lm}(x) = \int g(x, \theta, \phi) Y_{lm}(\theta, \phi) d\cos\theta d\phi \quad (39)$$

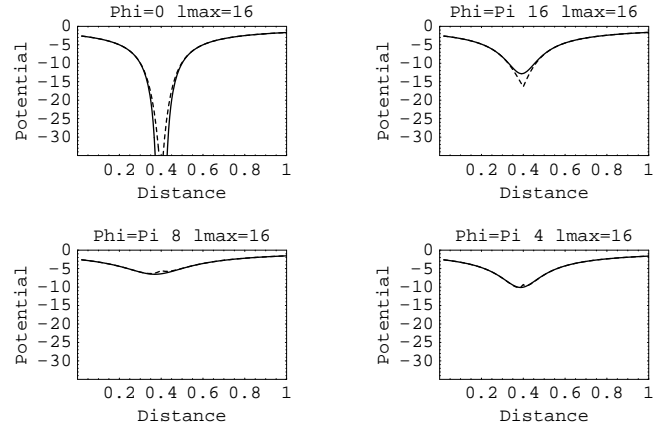
$$g(x, \theta, \phi) = \left[ 1 + e^{\frac{\beta}{\Theta} \sum_{l,m} u_{lm}(x) Y_{lm}(\theta, \phi) - \frac{1}{2} \beta \omega^2 x^2 \sin^2 \theta + \mu} \right]^{-1}$$

where  $l = 0, 1, \dots$  and  $m = -l, -l+1, \dots, l$ . Notice that  $u_{lm}$ ,  $\beta$  and  $\omega$  depend on  $b_{lm}$ . This system is completely equivalent to (30), but at least an iterative solution procedure is imaginable. After having fixed  $E$  and  $L$ , starting from an initial reasonable guess for  $b_{lm}(x)$ , one can compute  $u_{lm}(x)$  from (38) (1-dim. integral) (and  $\beta$  from (31)). Using this,  $b_{lm}(x)$  can be re-calculated from (39) (2-dim. integral) to improve the guess, and so until convergence via e.g. a simple Newton-Raphson method. As the starting point, it is convenient to take a high-energy configuration, where the kinetic contribution is expected to be much larger than the gravitational one, and a homogeneous cloud (“gas”) type of  $c(\mathbf{x})$  is very likely to solve (30). In particular, one can initiate from a totally symmetric configuration where  $b_{00}(x) = \Theta$  and  $b_{lm}(x) = 0$  for  $(l, m) \neq (0, 0)$ .

Clearly, actual calculations must be performed with a finite number of harmonics  $l_{\max}$ , i.e. the series (34) must be truncated. The effects of such a truncation are shown in Fig. 1. One sees the potential felt by one particle due to another one fixed at the position  $x = 0.4$  with  $\phi = 0$ . In (a), the first particle moves from  $x = 0$  to  $x = 1$  at fixed



(a) Fixed  $\phi = \pi/8$ , variable  $l_{\max}$



(b) Fixed  $l_{\max} = 16$ , variable  $\phi$

**Fig. 1.** Effects of truncation of the series (34) to the term of order  $l_{\max}$  (see text for details). Dashed and continuous lines represent the truncated potential and the Newtonian potential, respectively.

$\phi = \pi/8$  and the true potential is compared with the truncated one, with maximum number of included harmonics variable from 2 to 16. The latter case clearly reproduces the Newtonian force with a good degree of accuracy. However, the  $\phi$ -dependence must be considered also. This is shown in (b), where we fixed  $l_{\max} = 16$  and measured the potential varying the  $\phi$  of the second particle, keeping the first one fixed. It is clearly seen that the truncated potential works fine sufficiently far from the “probe” particle, while small deviations occur when the particles are too close. However this short-distance problem is substantially cured by our choice to deal with non-overlapping particles. A further hint about what should be the maximum order of harmonics to be included in the calculation comes from the study of the behaviour of  $b_{lm}(x)$  for typical solutions of (39), an example of which is reported in

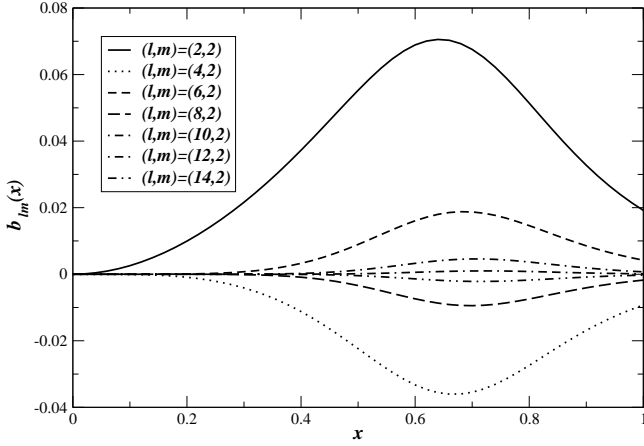


**Fig. 2.** Typical behaviour of the radial function  $b_{lm}(x)$  for different  $l$  ( $l$  even,  $2 \leq l \leq 14$ ) at fixed  $m = 2$ . This particular plot was obtained for  $E = -0.18$  and  $L = 0.44$ .

Fig. 2. One clearly sees that  $b_{lm}$  dies out as  $l$  increases, and that already for  $l = 14$  it is for all practical purposes zero.

Hence, we solved (39) taking  $l_{\max} = 16$ . We also excluded odd harmonics. Simple symmetry considerations suggest that exclusion of  $l = 1$  harmonics fixes the center of mass in the origin, while absence of higher-order odd harmonics prevents the formation of asymmetric structures (e.g. two clusters of different sizes lying at different distances from the origin). Their effects on the phase diagram will be studied elsewhere [29]. Finally, we measured energy and angular momentum in units of  $GN^2/R$  and  $(RGN^3)^{1/2}$ , respectively, and took  $\Theta = 0.02$  always<sup>5</sup>. The results of this analysis are reported in the next section.

### 3 Thermodynamics

#### 3.1 Phase diagram

We shall discuss here solutions of (39) obtained at fixed  $E$  and  $L$  in a slab of the  $(E, L)$  plane delimited by the lines  $E - L = 1$  and  $E = L$ . The entropy corresponding to each solution can be calculated via (27). Pure thermodynamic phases with one (macroscopic) equilibrium state can be discerned from phase coexistence regions by studying the Hessian of  $S$  in  $E$  and  $L$ , i.e.

$$\text{Hes}_{(E,L)}[S] = \det \begin{pmatrix} \partial_E^2 S & \partial_L \partial_E S \\ \partial_E \partial_L S & \partial_L^2 S \end{pmatrix} \quad (40)$$

In the microcanonical ensemble pure phases are characterized as having  $\text{Hes}_{(E,L)}[S] > 0$  (the entropy as a function of  $E$  and  $L$  is concave), while phase coexistence regions

<sup>5</sup> The  $\Theta$ -dependence of the results is an important issue. In fact, when  $\Theta$  is too large even the usual gravitational collapse transition does not take place because of particles jamming [15].

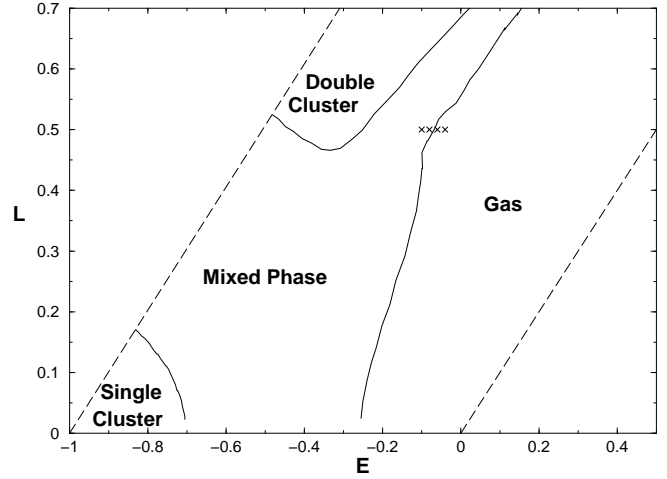


**Fig. 3.** Phase diagram in the  $(E, L)$ -plane. The dashed lines  $E - L = 1$  (left) and  $E = L$  (right) delimit the region where the Hessian was calculated. The four markers ( $\times$ ) correspond to the four situations described in Fig. 9.

have  $\text{Hes}_{(E,L)}[S] < 0$  [9, 26] (the entropy has a convex intruder). Mixed phases are characterized by negative specific heat and hence ensemble inequivalence. (The reader is referred to [9] for an introductory account on microcanonical thermostatics.) Fig. 3 shows the resulting global phase diagram of the system. In Fig. 4 one sees a sample of stationary distributions, together with the values of  $E$  and  $L$  at which they were obtained.

Results can be summarized as follows. For low angular momenta:

- at high energies (the kinetic term dominates), the solution of (39) is unique and is of the homogeneous cloud (“gas”) type; one finds that  $\text{Hes}_{(E,L)}[S] > 0$  and the corresponding (pure) phase is labeled as “gas” phase;
- at low energies, where gravity dominates, the solution of (39) is unique and of the single-cluster type (“single star”, e.g. Fig. 4a); correspondingly, one finds a pure thermodynamic state with  $\text{Hes}_{(E,L)}[S] > 0$ , which we call “single-cluster” state;
- in between these two regimes, one finds a phase coexistence region with  $\text{Hes}_{(E,L)}[S] < 0$  and negative specific heat, in which different solutions occur at each point  $(E, L)$  (“mixed phase”); here, single-cluster and gas type of solutions occur.

For slowly rotating systems one thus recovers a scenario that is similar to the usual gravitational collapse that is found in theories without angular momentum. For higher angular momenta (i.e. for a rapidly rotating system), instead:

- at high energies, the situation gas-type of solutions are obtained, and the situation is as in a. above;
- at low energies, the Hessian is positive and solutions of (39) are of double-cluster type (“double star”, e.g. Fig. 4b), and the corresponding phase, labeled “double cluster” is pure;

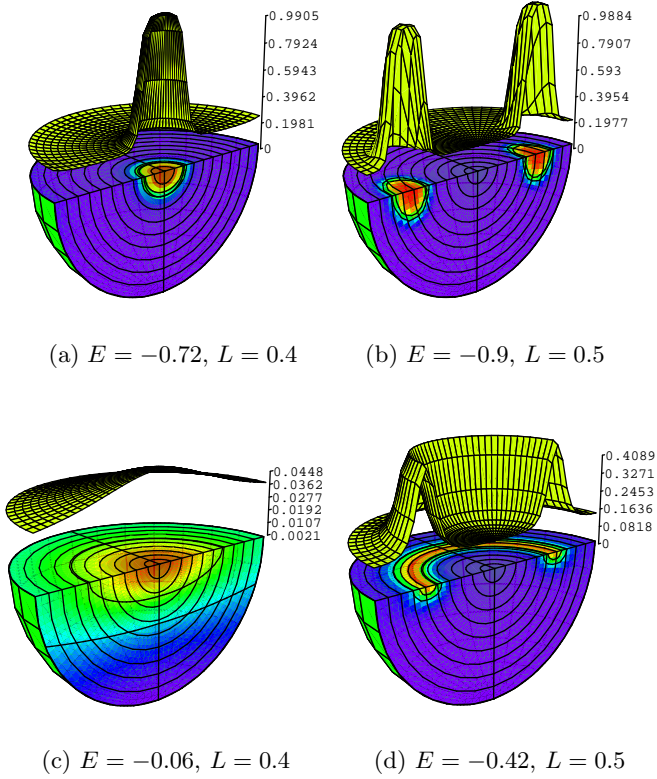


**Fig. 4.** Examples of stationary distributions  $c(\mathbf{x})$  occurring inside our spherical box. Shown are the contour plot and, above it, the density profile: (a) “single star”, (b) “double star”, (c) “disk”, (d) “ring”.

f. at intermediate energies, multiple solutions are found, both of double-cluster type and deformed gas-type. The latter in particular can be disks (e.g. Fig. 4c) or, if the angular momentum is high enough, rings (e.g. Fig. 4d). Correspondingly, the Hessian is negative and we have a phase coexistence region with negative specific heat.

The system thus turns out to have three pure phases (“gas”, “single star” and “double star”), separated by a large mixed phase. The occurrence of double-star-like solutions is the most remarkable effect of rotation. To get an idea of the coexistence of different solutions in the mixed phase, in Fig. 5 we plot the entropy for three different solutions (ring, single cluster, double cluster) in a range of energy at fixed  $L = 0.5$ . One sees that the entropy has a “convex intruder”, corresponding to the mixed phase and implying negative specific heat. The three solutions coexist in a whole range of energies, while at low energies, as evident from the phase diagram, the double-cluster solution only survives. The point where the rotationally asymmetric double-cluster solution bifurcates from the rotationally symmetric ring solution corresponds to the beginning of the mixed phase at  $L = 0.5$ . In the mixed phase: double-cluster and (deformed) gas type of configurations

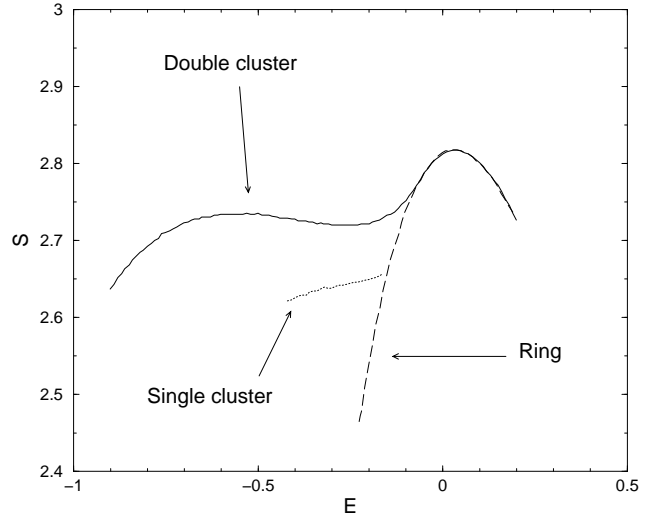


**Fig. 5.** Entropy as a function of energy at fixed  $L = 0.5$  for three different solutions, as shown. To make the convex intruder in the entropy (corresponding to the mixed phase) more evident, we subtracted the quantity  $(15/4)E$  from the entropy.

compete at high  $E$  and  $L$ ; single-cluster and gas compete at low  $L$ ; finally, single-cluster and double-cluster compete at intermediate values of  $L$ .

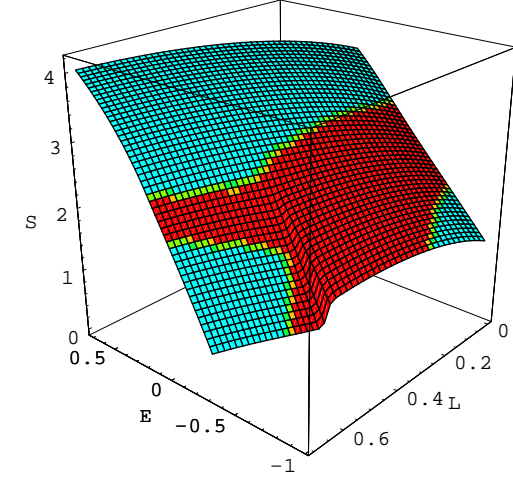
The crucial issue of stability (i.e. which of these configurations are actually entropy maxima in the space of  $c$ 's) will be dealt with in Sec. 3.4. For the moment, let it suffice to say that in the mixed phase, rotationally symmetric structures are unstable to perturbations that break rotational symmetry. Hence ring configurations, which also occur in the mixed phase, are not stable. Deformed gas configurations (e.g. disks or rings) that occur in the “gas” phase, e.g. close to the phase boundary, are stable. Before analyzing the different transitions that take place, we shall briefly discuss the important issue of negative specific heat.

### 3.2 Caloric curves, specific heat

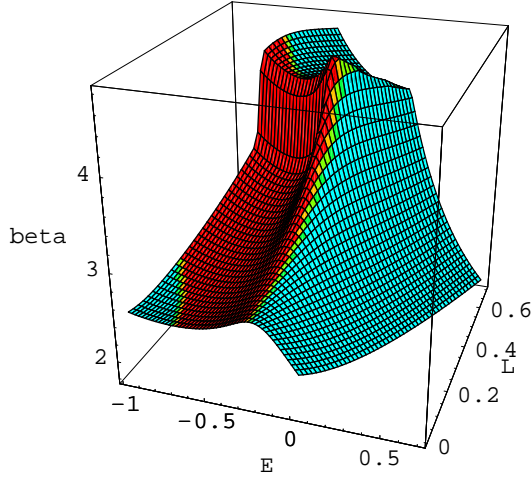
Once the solutions are obtained, the microcanonical entropy surface can be immediately calculated from (27). It is reported in Fig. 6 together with the  $\beta$ -surface, namely

$$\beta \equiv \beta(E, L) = \left( \frac{\partial S}{\partial E} \right)_{L=\text{constant}} \equiv \frac{1}{T} \quad (41)$$

representing the inverse microcanonical temperature as a function of energy and angular momentum. The central region in the entropy surface corresponds to the mixed phase and has  $\text{Hes}_{(E,L)}[S] < 0$ . Slices of the  $\beta$ -surface at different  $L$  (caloric curves) are shown in Fig. 7. One sees that  $\beta$  is increasing with  $E$  for a whole range of energies. This means that in that range  $\frac{\partial \beta}{\partial E} > 0$ , or equivalently that  $\frac{\partial E}{\partial T} < 0$ , i.e. that the specific heat is negative. Physically, if the system is heated (increase of total energy) its



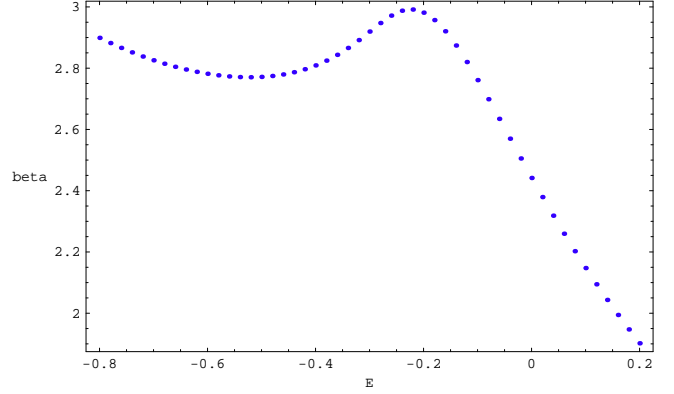
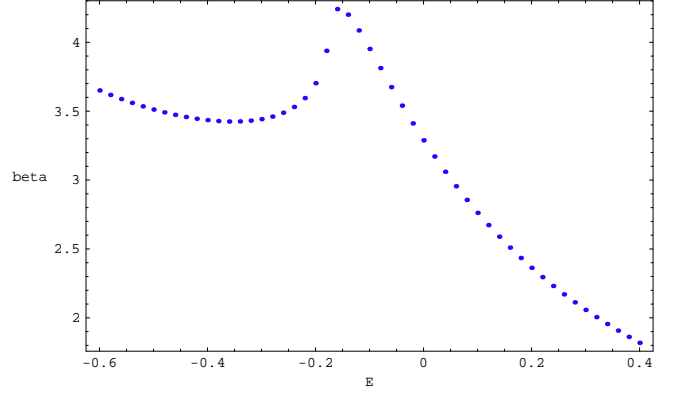
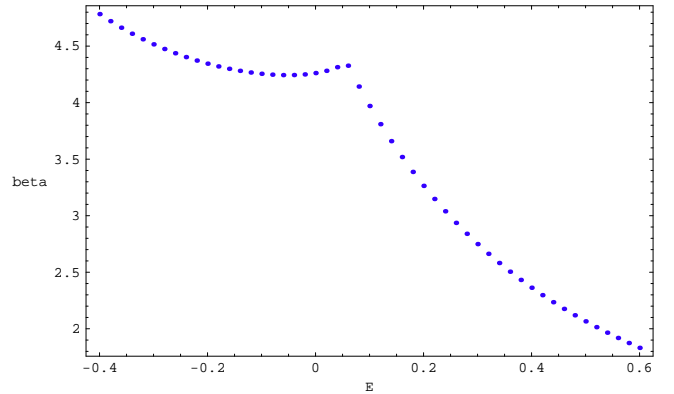
(a)



(b)

**Fig. 6.** (a) Microcanonical entropy  $S$  as a function of  $E$  and  $L$ . In the central region the Hessian  $\text{Hes}_{(E,L)}[S]$  is negative, signaling the separation of multiple phases (mixed phase). In the three clear regions, the Hessian is positive and pure thermodynamic phases (gas, single star, binary star, respectively) occur. (b) Behaviour of  $\beta = \partial_E S$  as a function of  $E$  and  $L$ .

temperature diminishes, and vice-versa if it loses energy its temperature increases. This is well-known to happen in stars. As they irradiate and release energy, they become hotter and hotter and contract. Such a behaviour, however, is not peculiar to self-gravitating systems, but is the generic signal of a phase separation in the microcanonical ensemble of finite systems [9, 14] and is not recoverable in the canonical ensemble, where the specific heat is proportional to energy fluctuations, i.e. non-negative definite.

(a)  $L = 0.2$ (b)  $L = 0.4$ (c)  $L = 0.6$ 

**Fig. 7.** Cross sections of the  $\beta$ -surface (inverse microcanonical temperature, caloric curves) at different angular momenta.



### 3.3 Phase transitions, symmetry breaking

We now turn to investigating the phase transitions. The low-angular-momentum collapse transitions are analogous to those discussed at length in the literature. A probably convenient order parameter to describe them is the density contrast, defined as the center-to-edge ratio of the particle density. We shall concentrate here on the rotational-symmetry-breaking transition to double-cluster solutions, which is the truly novel phenomenon introduced by rotation. A convenient order parameter to detect such a transition is

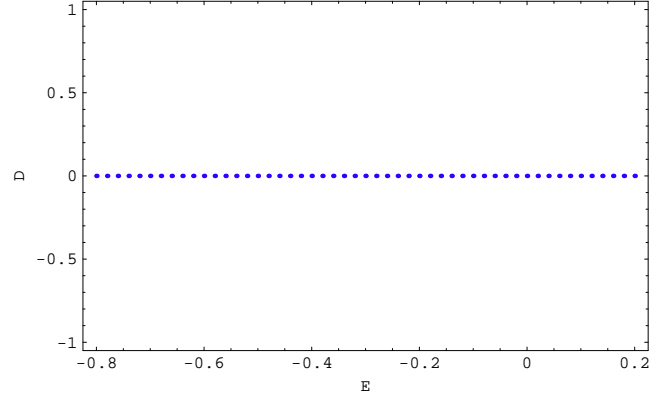
$$D = |I_{11} - I_{22}| \quad (42)$$

that is, the difference between 1 and 2 diagonal components of the inertia tensor (10). One expects  $D$  to be zero when the solution is rotationally-symmetric, and non-zero for a solution without rotational symmetry. The reason is physically clear. If  $L = 0$  (i.e. in absence of rotation) the system is necessarily isotropic ( $I_{11} = I_{22} = I_{33}$ ) and rotational symmetry cannot be broken. When  $L \neq 0$ , anisotropies may occur ( $I_{33} \neq I_{11}, I_{22}$ ) and one can have either rotationally-homogeneous ( $I_{11} = I_{22}$ ) or rotationally-heterogeneous ( $I_{11} \neq I_{22}$ ) solutions. The latter correspond to double clusters. (We remind the reader that the angular momentum is chosen to lie parallel to the 3-axis). In Fig. 8 we show explicitly that  $D$  actually behaves as a conventional order parameter for the rotational-symmetry-breaking transition (and the appearance of double clusters) by plotting it as a function of  $E$  at low and high angular momentum. By comparing Fig. 8b with the phase diagram the reader can notice that the transition occurs exactly at the phase boundary.

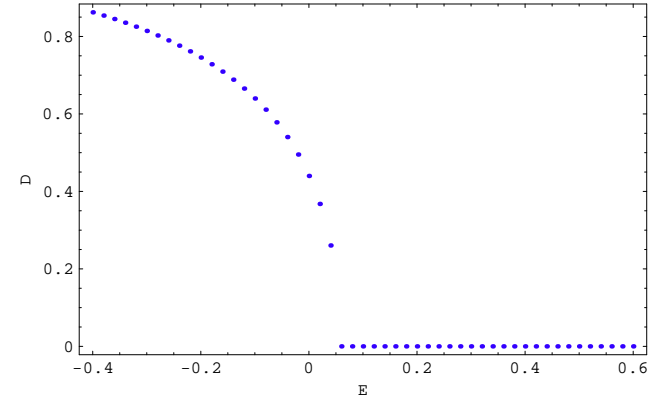
Another view of the same transition is given in Fig. 9. One sees the microcanonical entropy as a function of  $I_{11} - I_{22}$  at fixed  $L = 0.5$  and different energies. The four diagrams shown correspond to the four markers displayed across the gas-double cluster phase boundary in the phase diagram. The entropy is clearly seen to develop two peaks at non-zero values of  $I_{11} - I_{22}$ , corresponding to double clusters systems, with the two stars either aligned on the 1-axis or on the 2-axis, respectively. The fact that  $S$  becomes flat at the phase transition indicates that the transition is second-order. The minimum of  $S$ , occurring at  $I_{11} = I_{22}$ , corresponds to another, rotationally-symmetric solution of (30). In particular, it is a ring. This brings us to the problem of stability and clarifies further the structure of the mixed phase: at fixed  $E$  and  $L$ , the entropy in the  $c$  space has (at least) two maxima corresponding to double stars aligned on different axes. These are the only stable configurations.

### 3.4 Stability

Usually, the analysis of the (local) stability properties of the stationary points of the microcanonical entropy (27) at fixed mass, energy and angular momentum relies on the study the sign of second variation of the entropy. In



(a)  $L = 0.2$



(b)  $L = 0.6$

**Fig. 8.** Behaviour of the order parameter  $D = I_{11} - I_{22}$  as a function of energy  $E$  at fixed angular momentum  $L$ . At high  $L$ , breaking of rotational symmetry is signaled by a  $D \neq 0$ .

the reference frame of the principal inertia axes, where  $\mathbb{I}$  is diagonal, one can calculate such a variation explicitly. Omitting details of the lengthy calculation, one finds

$$\begin{aligned} \delta^2 S = & \frac{\beta}{\Theta^2} \int \frac{\delta c(\mathbf{x}) \delta c(\mathbf{x}')}{|\mathbf{x} - \mathbf{x}'|} d\mathbf{x} d\mathbf{x}' - \frac{1}{\Theta} \int \frac{(\delta c(\mathbf{x}))^2}{c(\mathbf{x})(1 - c(\mathbf{x}))} d\mathbf{x} + \\ & - \frac{2}{3\Theta^2} \left[ \int \delta c(\mathbf{x}) \log \frac{c(\mathbf{x})}{1 - c(\mathbf{x})} d\mathbf{x} \right]^2 + \\ & - \beta \sum_{a=1}^3 \frac{1}{I_{aa}} \left[ \int \delta c(\mathbf{x}) \omega^T \left( \frac{\delta \mathbb{I}^{(a)}}{\delta c(\mathbf{x})} \right) \right]^2 \quad (43) \end{aligned}$$

with  $\delta c(\mathbf{x})$  a mass-preserving perturbation ( $\int \delta c(\mathbf{x}) d\mathbf{x} = 0$ ).  $\mathbb{I}^{(a)} \equiv \mathbb{I}^{(a)}[c]$  stands for the  $a$ -th column of the inertia tensor  $\mathbb{I}$ . It is easy to show that for  $\beta \rightarrow 0$ , that is at sufficiently high energy where the kinetic term dominates, homogeneous gas-like stationary configurations are stable against any perturbation. It suffices to observe that when

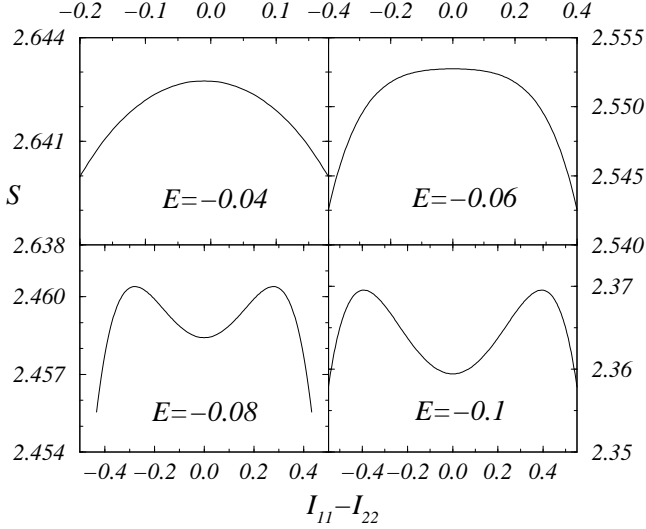


**Fig. 9.** Entropy as a function of  $I_{11} - I_{22}$  at  $L = 0.5$  and different values of  $E$ . The values of  $E$  and  $L$  for the four figures correspond to the four markers ( $\times$ ) shown in Fig. 3.

$\beta \rightarrow 0$  the above equation reduces to ( $\kappa > 0$  constant)

$$\delta^2 S(\beta \rightarrow 0) = -\kappa \int (\delta c(\mathbf{x}))^2 d\mathbf{x} < 0 \quad (44)$$

because  $c(\mathbf{x}) = \text{constant}$  and  $\delta c(\mathbf{x})$  is mass-preserving by assumption.

In a more general setting, the second variation of the entropy can be written as the quadratic form

$$\delta^2 S = \int f(\mathbf{x}) K(\mathbf{x}, \mathbf{x}') f(\mathbf{x}') d\mathbf{x} d\mathbf{x}' \quad (45)$$

where the kernel  $K$  is given by

$$\begin{aligned} K(\mathbf{x}, \mathbf{x}') = & -\beta \frac{\delta^2 \Phi}{\delta c(\mathbf{x}) \delta c(\mathbf{x}')} - \frac{1}{\Theta} \frac{\delta(\mathbf{x} - \mathbf{x}')}{c(\mathbf{x})(1 - c(\mathbf{x}'))} + \\ & -\frac{2\beta^2}{3} \left[ \frac{\delta \Phi}{\delta c(\mathbf{x})} - \frac{1}{2} \omega^T \frac{\delta \mathbb{I}}{\delta c(\mathbf{x})} \omega \right] \left[ \frac{\delta \Phi}{\delta c(\mathbf{x}')} - \frac{1}{2} \omega'^T \frac{\delta \mathbb{I}}{\delta c(\mathbf{x}')} \omega' \right] + \\ & -\frac{\beta}{2} \omega^T \left[ \frac{\delta \mathbb{I}}{\delta c(\mathbf{x}')} \mathbb{I}^{-1} \frac{\delta \mathbb{I}}{\delta c(\mathbf{x})} + \frac{\delta \mathbb{I}}{\delta c(\mathbf{x})} \mathbb{I}^{-1} \frac{\delta \mathbb{I}}{\delta c(\mathbf{x}')} \right] \omega \end{aligned} \quad (46)$$

and where as before  $\Phi$  stands for the Newtonian potential. Stability analysis is then equivalent to studying the eigenvalue problem for  $K$ , namely

$$\int K(\mathbf{x}, \mathbf{x}') f(\mathbf{x}') d\mathbf{x}' = \lambda f(\mathbf{x}) \quad (47)$$

(see e.g. [30]). From a mathematical viewpoint, this task is extremely sophisticated. We shall therefore limit ourselves here to discuss the stability of rotationally-symmetric configurations against perturbations that break rotational symmetry, deferring the reader to a later publication for a more complete analysis of the stability problem.

From the analysis of the preceding section, and in particular from Fig. 9, it stems that rotationally symmetric configurations become unstable against perturbations that break rotational symmetry at sufficiently high angular momenta and energies. Two rotationally asymmetric solutions of (39) bifurcate continuously from the rotationally symmetric state. At least for what concerns this class of perturbations, it is safe to claim that rotationally symmetric structures are stable up to the phase boundary. Among them, one finds gas-like homogeneous configurations, and deformed-gas configurations (i.e. disks and rings). At the phase boundary, solutions with  $D = 0$  become entropy minima at least along one direction in the  $c$  space, and are no longer stable against rotational symmetry breaking. Instead, the only stable configurations in the mixed phase at high enough angular momentum are double-cluster like ( $D \neq 0$ ).

A more technical argument that supports this conclusion is the following. Let (see (30))

$$G[c] = (1 + e^{\frac{\beta}{\Theta} U(\mathbf{x}) - \frac{1}{2} \beta (\omega \times \mathbf{x})^2 + \mu})^{-1} - c(\mathbf{x}) \quad (48)$$

It is easy to show<sup>6</sup> that

$$\left[ \frac{\delta^2 S}{\delta c(\mathbf{x}) \delta c(\mathbf{x}')} \right]_{G[c]=0} = \gamma \left[ \frac{\delta G}{\delta c(\mathbf{x}')} \right]_{G[c]=0} \quad (49)$$

with  $\gamma > 0$ , i.e. that the second functional derivative of the entropy evaluated at the stationary point vanishes together with the functional derivative of  $G$  evaluated at the same point, and that the two have the same sign. This implies that the stability analysis can be reduced to the study of the sign of  $\delta G / \delta c$ . However, the latter problem is dealt with when applying the Newton-Raphson method to solve (30). Starting from high energies, in order to provoke a rotationally asymmetric solution an appropriate external field (in this case, it is related to the order parameter discussed in the previous subsection) must be added to  $G$  as an external perturbation. A bifurcation of a rotationally-asymmetric solution implies a change of sign of  $\delta G / \delta c$ , meaning that the rotationally symmetric one has become unstable to that particular perturbation. Hence, the instability-onset line for perturbations that break rotational symmetry numerically coincides with the phase boundary between the “gas” and the “double cluster” phases, where  $\text{Hes}_{(E,L)}[S] = 0$ , displayed in the phase diagram.

## 4 Outlook and final remarks

We have presented an analysis of the equilibrium properties of a self-gravitating and rotating gas using a mi-

<sup>6</sup> It is sufficient to note that

$$\frac{\delta S}{\delta c(\mathbf{x})} = \frac{1}{\Theta} \log \frac{(1 - c(\mathbf{x}))(c(\mathbf{x}) + G[c])}{c(\mathbf{x})(1 - c(\mathbf{x}) - G[c])}$$

Taking the functional derivative of this expression with respect to  $c(\mathbf{x}')$  and evaluating it at the stationary point, one finds (49) with  $\gamma = [\Theta c(\mathbf{x})(1 - c(\mathbf{x}))]^{-1}$ .

crocanonical mean-field approach. Our main result concerns the spontaneous breaking of the rotational symmetry, which takes place at high angular momentum and gives rise to non-trivial density profiles, e.g. “double stars”: a rapidly rotating  $N$ -body system kept together by gravitation only at equilibrium spontaneously organizes in two distinct dense clusters, provided the ratio between rotational and gravitational energy is sufficiently high and the total energy is not too large. We have derived the global phase diagram of the model and discussed the related thermodynamic picture, providing a phenomenological description of the phase transitions occurring and analyzing the stability of high-energy rotationally-symmetric equilibrium states against perturbations that break rotational symmetry, showing that non-trivial rotationally symmetric solutions such as rings become unstable in the mixed (phase coexistence) region. To our knowledge, these results constitute the most complete equilibrium description of a self-gravitating and rotating system to date. To conclude, we would like to put forward some final remarks and open problems.

- i. While it is certainly possible to improve on the results presented here by increasing the maximum order of the even harmonics included in the calculation, we do not expect any major qualitative difference with the picture we describe here ( $l_{\max} = 16$ ). The inclusion of odd harmonics would instead lead to the formation of asymmetric double clusters, and to a more complete phase diagram and a full classification of the different possible equilibrium configurations as a consequence. This issue will be treated elsewhere [29].
- ii. Our results stem from a mean-field analysis, in which particle-particle correlations are completely neglected.
- iii. We have not studied how our results depend on  $\Theta$ , namely on the average density of the system. We mentioned that this is an important issue, certainly worth to be investigated with great care.
- iv. A general stability analysis requires, as we said, the study of the eigenvalue problem for  $K$ , Eq. (46). The most interesting open question is that of marginal stability, that is solutions of (47) with zero eigenvalue. However, the approach we discussed in the last section, connecting the stability analysis to the bifurcation analysis, describes correctly the stability of the different states against perturbations that break rotational symmetry (within the included number of harmonics).
- v. From a physical point of view, it is known that energy and angular momentum are possibly not the only conserved quantities to be taken into account if one wants to recover some observational features of e.g. galaxies [31].
- vi. Of course, we have dealt with equilibrium properties exclusively, and provided a kind of classification of the different possible states of the system. This clearly leaves open many important questions concerning dynamics and relaxation mechanisms, which are believed to be particularly subtle in self-gravitating systems [21].

On a more general level, the equilibrium properties of non-extensive Hamiltonian systems (self-gravitating and rotating systems being the most important example) can be well described by Boltzmann’s principle (4). We would finally like to stress the potentialities of the method presented here for studying the equilibrium properties of systems with long-range (see footnote 1) forces. Its basic ingredients are: (a) microcanonical statistics and (b) a series expansion of the potential using a proper basis set. This same scheme can easily be modified to work with other types of long-range potentials (e.g. Coulomb or Yukawa). In the light of this last remark, self-gravitating and rotating systems (for which the use of “corrective” techniques such as the Kac-Uhlenbeck-Hemmer method [32] is substantially not helpful in clarifying its complex thermodynamic structure) should be considered as a fundamental testing ground for techniques to analyze the statistical equilibrium properties of systems with long-range interactions.

**Acknowledgments.** We wish to thank P.H. Chavanis and O. Fliegans for important comments, and the Deutsche Forschungsgemeinschaft (DFG) for financial support. We also acknowledge useful discussions with the participants of the conference on “Dynamics and Thermodynamics of Systems with Long Range Interactions” (Les Houches, February 2002).

## References

1. L.D. Landau and E.M. Lifshitz. *Statistical Physics*. Butterworth-Heinemann, Oxford, 1996.
2. D. Lynden-Bell and R. Wood. The gravo-thermal catastrophe in isothermal spheres and the onset of red-giant structure for stellar systems. *Mon. Not. R. Astron. Soc.* **138** 495 (1968)
3. W. Thirring. Systems with negative specific heat. *Z. f. Phys.* **235** 339 (1970)
4. D.H.E. Gross and H. Massmann. Statistical fragmentation of very hot nuclei, complete microcanonical approach. *Nucl. Phys. A* **471** 339c (1987)
5. D.H.E. Gross and M. Madjet. Microcanonical vs canonical thermodynamics. Preprint cond-mat/9611192
6. D. Lynden-Bell. Negative specific heat in astronomy, physics and chemistry. *Physica A* **263** 293 (1999) Preprint cond-mat/9812172.
7. D.H.E. Gross and R. Heck. What is wrong with the Bethe formula? - Measurable differences between the grand-canonical and microcanonical ensemble. *Phys. Lett.B* **318** 405 (1993)
8. P.A. Hervieux and D.H.E. Gross. Evaporation of hot mesoscopic metal cluster. *Z. Phys. D* **33** 295 (1995)
9. D.H.E. Gross. *Microcanonical thermodynamics: Phase transitions in “Small” systems*, volume 66 of *Lecture Notes in Physics*. World Scientific, Singapore, 2001.
10. J. Barre, D. Mukamel and S. Ruffo. Inequivalence of ensembles in a system with long range interactions. *Phys. Rev. Lett.* **87** 030601 (2001) Preprint cond-mat/0102036.
11. G. Gallavotti. *Statistical Mechanics*. Texts and Monographs in Physics. Springer, Berlin, 1999.

12. H.J. de Vega, N. Sanchez, and F. Combes. Self-gravity as an explanation of the fractal structure of the interstellar medium. *Nature* **383** 66 (1996)
13. H.J. de Vega, N. Sanchez, and F. Combes. The fractal structure of the universe: a new field theory approach. *Astrophys. J.* **500** 8 (1998)
14. D.H.E. Gross. Geometric foundation of thermo-statistics, phase transitions, second law of thermodynamics, but without thermodynamic limit. *Phys. Chem. Chem. Phys.* **4** 863 (2002). Preprint cond-mat/0201235.
15. T. Padmanabhan. Statistical mechanics of gravitating systems. *Phys. Rep.* **188** 286 (1990)
16. P.H. Chavanis, C. Rosier, and C. Sire. Thermodynamics of self-gravitating systems. Preprint cond-mat/0107345.
17. M. Cerruti-Sola, P. Cipriani, and M. Pettini. On the clustering phase transition in self-gravitating  $N$ -body systems. *Astron. & Astrophys.* **328** 339 (2001)
18. P.H. Chavanis. Gravitational instability of finite isothermal spheres. *Astron. & Astrophys.* **381** 340 (2002)
19. V.A. Antonov. *Vest. Leningrad Univ.* **7** 135 (1962). Translated in IAU Symposium **113** 525 (1995).
20. H.J. de Vega and N. Sanchez. Statistical mechanics of the self-gravitating gas: I. Thermodynamic limit and phase diagrams. *Nucl. Phys. B* **625** 409 (2002)
21. D. Lynden-Bell. Statistical mechanics of violent relaxation in stellar systems. *Mon. Not. R. Astron. Soc.* **136** 101 (1967)
22. S. Chandrasekhar. *Ellipsoidal figures of equilibrium*. Yale University Press, New Haven, 1969.
23. A. Burkert and P. Bodenheimer. Multiple fragmentation in collapsing protostars. *Mon. Not. R. Astron. Soc.* **264** 798 (1993)
24. O. Fliegans and D.H.E. Gross. Effect of angular momentum on equilibrium properties of a self-gravitating system. *Phys. Rev. E* **65** 046143 (2002). Preprint cond-mat/0102062.
25. V. Laliena. The effect of angular momentum conservation in the phase transitions of collapsing systems. *Phys. Rev. E* **59** 4786 (1999) Preprint cond-mat/9806241.
26. D.H.E. Gross and E.V. Votyakov. Phase transitions in “small” systems. *Eur. Phys. J. B* **15** 115 (2000) Preprint cond-mat/9911257.
27. E.V. Votyakov, H.I. Hidmi, A. De Martino and D.H.E. Gross. Microcanonical mean-field thermodynamics of self-gravitating and rotating systems. *Phys. Rev. Lett.* **89** 031101 (2002). Preprint cond-mat/0202140.
28. H.W. Wyld. *Mathematical methods for physicists*. Benjamin Inc., Reading, 1976.
29. In preparation.
30. T. Padmanabhan. Antonov instability and gravothermal catastrophe – Revisited. *Astrophys. J. Suppl. Series* **71** 651 (1989)
31. G. Contopoulos. A third integral of motion in a galaxy. *Z. Astrophys.* **49** 273 (1960)
32. M. Kac, G. E. Uhlenbeck and P. C. Hemmer. On the van der Waals theory of the vapor-liquid equilibrium I. Discussion of a one-dimensional model. *J. Math. Phys.* **4** 216 (1963)